Inorg. Chem. **2003**, *42*, 4909–4917

Stoichiometric and Catalytic Activation of the α- and β-2,3,4-Tri-*O*-Acetyl-5-Thioxylopyranosyl Bromide Inside the Cavity of the $Pd_3(dppm)_3(CO)^{2+}$ Cluster

David Brevet,[1a] Yves Mugnier,*[,1a] Frédéric Lemaître,[1a,c] Dominique Lucas,[1a] Soth Samreth,[1b] and Pierre D. Harvey*[,1c]

Laboratoire de Synthèse et d'Electrosynthèse Organométalliques, CNRS UMR 5632, Faculté des Sciences Gabriel, Université de Bourgogne, 6 Boulevard Gabriel, 21000 Dijon, France, Laboratoire Fournier, 50 rue de Dijon 21121 Daix, and Département de Chimie, Université de Sherbrooke, Sherbrooke, Québec, Canada J1K 2R1

Received December 17, 2002

The title cluster (Pd_3^{2+}) exhibits a pronounced affinity for Br^- ions to form the very stable $Pd_3(Br)^+$ adduct. Upon a 2-electron reduction, a dissociative process occurs generating Pd_3^0 and eliminating Br^- according to an ECE mechanism (electrochemical, chemical, electrochemical). At a lower temperature (i.e. –20 °C), both ECE and EEC processes operate. This cluster also activates the C–Br bond, and this work deals with the reactivity of Pd_3^{2+} with 2,3,4-tri-*O*-acetyl-5-thioxylopyranosyl bromide (Xyl–Br), both α- and β-isomers. The observed inorganic product is $Pd_3(Br)^+$ again, and it is formed according to an associative mechanism involving $Pd_3^{2+}\cdots$Xyl–Br host–guest assemblies. In an attempt to render the C–Br bond activation catalytic, these species are investigated under reduction conditions at two potentials (–0.9 and –1.25 V vs SCE). In the former case, the major product is Xyl–H, issued from a radical intermediate Xyl• abstracting an H atom from the solvent. Evidence for Xyl• is provided by the trapping with TEMPO (2,2,6,6-tetramethyl-1-piperidinyloxy) and DMPO (5,5′-dimethylpyrroline-N-oxyde). In the second case, only one product is observed, 3,4-di-*O*-acetyl-5-thioxylal, which is issued from the Xyl^- intermediate anion.

Introduction

C−X bond activation is a very important process involved in many organic reactions.[2] An obvious example stressing its importance is certainly the Heck reaction.[3] The title cluster exhibits a pronounced affinity toward anionic species (Figure 1), and we recently reported the heterolytic activation of the alkyl C−X bonds (X = Br, I) which proceeds efficiently via an electrochemical induction of the Lewis acid cluster Pd_3^{2+}, as a $CF_3CO_2^-$ salt.[4]

The inorganic product is the corresponding adduct $Pd_3(X)^+$ (X = Br, I), while the organic intermediate "R^+" can be trapped with an appropriate nucleophile such as phenol to generate the corresponding dissymmetric ether. In a parallel study,[5] we investigated in detail the electrochemical behavior of the title cluster in the presence of I^- ions, allowing the establishment of the mechanisms by which the $Pd_3(I)^+$ is reduced. The generation of the highly reactive carbocation provides an opportunity to explore applications in organic chemistry, but also the three different oxidation

* To whom correspondence should be addressed. E-mail: pharvey@courrier.usherb.ca (P.D.H.); Yves.Mugnier@u-bourgogne.fr (Y.M.). Phone: (819) 821-2005 (P.D.H.). Fax: (819) 821-8017 (P.D.H.). Phone and fax: (33) 3 80 39 60 91 (Y.M.).

(1) (a) Université de Bourgogne. (b) Laboratoire Fournier. (c) Université de Sherbrooke.

(2) (a) Kulawiec, R. J.; Crabtree, R. H. *Coord. Chem. Rev.* **1990**, *99*, 89. (b) Stille, J. K.; Kriesler, S. Y. L. *Acc. Chem. Res.* **1977**, *10*, 434. (c) *Organometallic Mechanisms and Cata1ysis*; Kochi, J. K., Ed.; Academic Press: New York, 1978; p 156. (d) *Comprehensive Organometallic Chemistry II*; Abel, E. W., Stone, F. G. A., Wilkinson, G., Eds.; Pergamon: Oxford, U.K.; 1995; Vol.12, p 161. (e) *Principles and Applications of Organotransition Metal Chemistry*; Collman, J. P., Hegedus, L. S., Norton, J. R., Eds.; University Science Books: Mill Valley, CA, 1987. (f) *Applied Homogeneous Catalysis with Organometallic Compounds*; Cornils, B., Hermann, W. A., Eds.; Wiley: Weinheim, Germany, 1999. (g) *Transition Metal Reagents and Catalysts: Innovations in Organic Synthesis*; Tsuji, J., Ed.; Wiley: Chichester, U.K., 2000.

(3) Beletskaya, I. P.; Cheprakov, A. V. *Chem. Rev.* **2000**, *100*, 3009 and references therein.

(4) Brevet, D.; Lucas, D.; Cattey, H.; Lemaître, F.; Mugnier, Y.; Harvey, P. D. *J. Am. Chem. Soc.* **2001**, *123*, 4340.

(5) Lemaître, F.; Brevet, D.; Lucas, D.; Vallat, A.; Mugnier, Y.; Harvey, P. D. *Inorg. Chem.* **2002**, *41*, 2368.

10.1021/ic026279x CCC: $25.00
Published on Web 07/08/2003

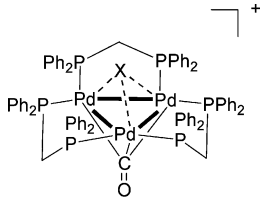

$Pd_3(dppm)_3(CO)(X)^+$

$X^- = CF_3CO_2^-, Br^-$

Figure 1. Drawing of the $Pd_3(dppm)_3(CO)(X)^+$ clusters (if $X^- = PF_6^-$, the cavity of the cluster can be considered as empty and the cluster is best described as $Pd_3(dppm)_3(CO)^{2+}$).

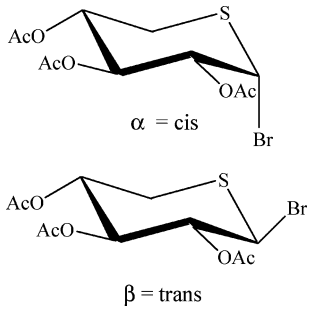

Figure 2. Drawings of the 2,3,4-tri-*O*-acetyl-5-thioxylopyranosyl bromide substrates (Xyl−Br).

states of the Pd_3^{n+} ($n = 0, 1, 2$) can be exploited for this same purpose.

We are currently exploring the electrochemical activation of different glycoside bromides using this cluster. Although the use of glycosyl bromides as an effective glycosyl donors in the glycosylation reactions has been extensively studied, the development of new methods for glycoside synthesis is an area of current interest.[6,7] One application is the reduction of α- or *β*-2,3,4-tri-*O*-acetyl-5-thioxylopyranosyl bromide (Figure 2).[8]

We now wish to report both stoichiometric and catalytic reactivity of the Pd_3^{2+} species and its reduced form, Pd_3^+ and Pd_3^0, toward Xyl−Br. Interestingly, the overvoltage for the catalytic reduction of Xyl−Br is reduced by 0.55 V (for Pd_3^+) or 0.9 V (for Pd_3^0) with respect to Xyl−Br alone without the presence of clusters. During the course of this study, the reduction mechanism for the $Pd_3(Br)^+$ adduct was investigated in order to provide a better understanding of the activation mechanism of Xyl−Br by the Pd_3^{n+} ($n = 0$, 1, 2) species.

Experimental Section

Materials. The $[Pd_3(dppm)_3(CO)](PF_6)_2$ and $[Pd_3(dppm)_3(CO)](CF_3CO_2)_2$ complexes were prepared according to literature procedures.[9] Tetrahydrofuran (THF) was distilled under Ar over Na and benzophenone. The supporting electrolyte used in each experiment was Bu_4NPF_6 (Aldrich). The salt was recrystallized twice in ethanol and dried at 80 °C for at least 2 days before use. The Bu_4NBr (Aldrich) was dried at 80 °C at least 2 days before use. The α- and *β*-Xyl−Br were provided by the Laboratoire Fournier and were synthesized according to published methods.[10]

The EPR measurements were carried out on a Bruker ESP 300 spectrometer; field calibration was made with DPPH ($g = 2.0037$). NMR spectra were measured at 293 K on a Bruker AVANCE DRX 500 spectrometer (^{1}H NMR, 500.13 MHz; ^{31}P NMR, 202.46 MHz; ^{13}C NMR, 125.77 MHz). The reference was the residual nondeuterated solvent. UV−vis absorption spectra were recorded on a Varian CARY 1 spectrometer. GC-MS data were collected on a Hewlett-Packard 6890 series apparatus.

Electrochemical Experiments. All manipulations were performed using Schlenk techniques in an atmosphere of dry oxygen-free nitrogen gas. The supporting electrolyte was degassed under vacuum before use and then solubilized at a concentration of 0.2 M. For cyclic voltammetry experiments, the concentration of the analyte was nearly 10^{-3} M. Voltammetric analyses were carried out in a standard three-electrode cell with a Tacussel PRT 30-0.1 unit cell. The reference electrode was a saturated calomel electrode (SCE) separated from the solution by a sintered glass disk. The auxiliary electrode was a platinum wire. For all voltammetric measurements, the working electrode was a vitreous carbon electrode ($\phi = 3$ mm). In these conditions, when operating in THF, the formal potential for the ferrocene$^{+/-}$ couple is found to be +0.56 V versus SCE. The controlled potential electrolysis was performed with an Amel 552 potentiostat coupled with an IG5-N electronic integrator. The electrolyses were performed in a three-compartment cell equipped with fritted glass separators of medium porosity. A carbon gauze was used as the working electrode, a platinum plate as the counter electrode, and a saturated calomel electrode as the reference electrode.

Computer Modeling. Computer modeling was performed using the commercially available program called PC-Model version 7.0 which uses the MMX parameters. The modeled $Pd_3(dppm)_3(CO)$ structure exhibits $d(Pd_2) = 2.625$ Å, (Pd−P) = 2.29 Å, and d(P−C) = 1.77 Å, close to reported X-ray data ($d(Pd_2) = 2.60$ Å, d(Pd−P) = 2.31 Å, d(P−C) = 1.77 Å).[11]

Synthesis of 2,3,4-Tetra-*O*-acetyl-xylotetrahydrothiopyrane (Xyl−H). Electrolysis at the Potential of Peak A. The cell was loaded with dry THF (10 mL), Bu_4NPF_6 (0.8 g), $[Pd_3(dppm)_3(CO)]$-

(6) (a) Garegg, P. J. *Adv. Carbohyd. Res. Bi.* **1997**, *52*, 179. (b) Toshima, K.; Tatsuta K. *Chem. Rev.* **1993**, *93*, 1503.

(7) (a) Only a few electrosyntheses of glycoside have been described and concern the *O*-glycosylation reaction starting from *S*-glycoside[7b−f] or glycosyl halide[7g] or glycosyl alkoxides[7h] as glycoside acceptor. Recently, efficient electrochemical *N*-glycosylation has been reported.[7i] (b) Balavoine, G.; Gref, A.; Fischer, J. C.; Lubineau, A. *Tetrahedron Lett.* **1998**, *40*, 5761. (c) Amatore, C.; Jutand, A.; Mallet, J. M.; Meyer, G.; Sinaÿ, P. *J. Chem. Soc., Chem. Commun.* **1990**, 718. (d) Mallet, J. M.; Gilbert, G.; Yvelin, F.; Jutand, A.; Amatore, C.; Sinaÿ, P. *Carbohydr. Res.* **1993**, *244*, 237. (e) Amatore, C.; Jutand, A.; Meyer, G.; Bourhis, P.; Machetto, F.; Mallet, J. M.; Sinaÿ, P.; Tabeur, C.; Zhang, Y. M. *J. Appl. Electrochem.* **1994**, *24*, 725. (f) Balavoine, G.; Berteina, S.; Gref, A.; Fischer, J. C.; Lubineau, A. *J. Carbohydr. Chem.* **1995**, *14*, 1217. (g) Rondini, S.; Mussini, P. R.; Sello, G.; Vismara, E. *J. Electrochem. Soc.* **1998**, *145*, 1108. (h) Noyori, R.; Kirimoto, I. *J. Org. Chem.* **1986**, *51*, 4320. (i) Nokami, J.; Osafune, M.; Ito, Y; Miyake, F.; Sumida, S. I.; Torii, S. *Chem. Lett.* **1999**, 1053.

(8) (a) Research in this area is intensive[8b] because its derivatives belong to a class of compounds called α-D-xylopyranosides, some of which present oral antithrombotic activity.[8c−e] (b) Horton, D.; Wander, J. D. In *The Carbohydrates Chemistry and Biochemistry*; Pigman, W., Horton, D., Eds.; Academic: New York, 1980; Vol. IB, p 799. (c) Bellamy, F.; Horton, D.; Pacart, F.; Millet, J.; Samreth, S.; Chazan, J. B. *J. Med. Chem.* **1993**, *36*, 898. (d) Samreth, S.; Bellamy, F.; Millet, J.; Barberousse, V.; Renault, P.; Bajgrowick, J. EPO, 365397, 1991; *Chem. Abstr.* **1991**, *114*, 122964k. (e) Barberousse, V.; Legendre, C.; Samreth, S.; Edgar, A. U.S. Patent 6291433, 2001.

(9) (a) Manojlovic-Muir, L. J.; Muir, K. W.; Lloyd, B. R.; Puddephatt, R. J. *J. Chem. Soc., Chem. Commun.* **1983**, 1336. (b) Lloyd, B. R.; Puddephatt, R. J. *Inorg. Chim. Acta* **1984**, *90*, L77.

(10) (a) Whistler, R. L.; Van Es, T. *J. Org. Chem.* **1963**, *28*, 2303. (b) Baudry, M.; Bouchu, M. N.; Descotes, G.; Praly, J. P.; Bellamy, F. *Carbohydr. Res.* **1996**, *282*, 237.

(11) Provencher, R.; Aye, K. T.; Drouin, M.; Gagnon, J.; Boudreault, N.; Harvey, P. D. *Inorg. Chem.* **1994**, *33*, 3689.

$(PF_6)_2$ (15 mg, 0.008 mmol), and Xyl−Br (62 mg, 0.175 mmol) under N_2. The two electrodes consist of a carbon gauze cathode and a platinum wire as counter electrode. The electrolysis was performed at room temperature at a constant potential of −0.95 V versus SCE, and 20 F/mol was passed through the solution. The solution was concentrated and taken up with ethyl acetate. The supporting electrolyte was precipitated with Et_2O. The mixture was filtered and the organic phase evaporated. Chromatography on a silica gel column (toluene/ethyl acetate 9/1 v/v) yielded the unsaturated sugar 3,4-di-*O*-acetyl-5-thioxylal (12%) and Xyl−H (79%). The 3,4-di-*O*-acetyl-5-thioxylal species was identified by comparison with the spectroscopic data previously reported in the literature.[12] Analyses for Xyl−H are as follows. ^{1}H NMR (DMSO-d_6): δ (ppm) 5.04 (t, 1 H, H-3, ^3J(H-3, H-2) = 10.9 Hz), 4.82−4.90 (m, 2 H, H-2, H-4), 2.71−2.87 (m, 4 H, H-1, H-1′, H-5, H-5′), 1.97 (s, 9 H, 3 CH_3). ^{13}C NMR (DMSO-d_6): δ (ppm) 169.3, 169.4 (CdO), 73 (C3), 72.4 (C2, C4), 29.3 (C1,C_5), 20.6 (CH_3). Anal. Calcd for $C_{11}H_{16}O_6S$: C, 47.83%; H, 5.80%; S, 11.59%. Found: C, 47.94%; H, 5.98%; S, 11.29%.

Electrolysis at the Potential of Peak A in the Presence of 5,5′-Dimethyl-1-pyrroline-*N*-oxide (DMPO) or 2,2,6,6-Tetramethylpiperidin-1-oxyl (TEMPO). The same conditions as those for the synthesis of Xyl−H were applied, except that DMPO or TEMPO was added prior to electrolysis (quantity equimolar to Xyl−Br). The same purification procedure was used (column chromatography solvent = hexane/ethyl acetate 85/15 v/v), which allowed isolation of both stereoisomers of the TEMPO adduct (2,2,6,6-tetramethylpiperidin-1-oxyl 2,3,4-tri-*O*-acetyl-5-thioxylopyranoside). Yield: 58% (α/β = 6/4). Analyses for 2,2,6,6-tetramethylpiperidin-1-oxyl 2,3,4-tri-*O*-acetyl-5-thioxylopyranoside follow. ^{1}H NMR ($CDCl_3$): α-isomer δ (ppm) 5.36−5.43 (m, 2 H, H-2, H-3), 5.16 (d, 1 H, H-1, ^3J(H-1, H-2) = 3.7 Hz), 5.08−5.13 (m, 1 H, H-4), 2.72−2.86 (m, 2 H, H-5, H-5′), 2.04 (s, 3 H, CH_3), 2.03 (s, 3 H, CH_3), 2.01 (s, 3 H, CH_3), 1.53 (m, 2 H, CH_2), 1.51 (m, 2 H, CH_2), 1.46 (m, 2 H, CH_2), 1.22 (s, 12 H, 4 CH_3); β-isomer δ (ppm) 5.35 (t, 1 H, H-3, ^3J(H-3, H-2) = 9.3 Hz), 5.11 (d, 1 H, H-1, ^3J(H-1, H-2) = 9.4 Hz), 5.06 (t, 1 H, H-2, ^3J(H-1, H-2) = 9.4 Hz), 4.95−5.00 (m, 1 H, H-4), 2.44−2.86 (m, 2 H, H-5, H-5′), 2.05 (s, 3 H, CH_3), 2.02 (s, 3 H, CH_3), 1.99 (s, 3 H, CH_3), 1.42−1.55 (m, 6 H, CH_2), 1,15 (s, 12 H, 4 CH_3). MS (EI): m/z = 432 (M + 1), 275 (M − TEMPO), 215 (M − TEMPO − CH_3CO_2H), 156 (M − Xyl).

Synthesis of 3,4-Di-*O*-acetyl-5-thioxylal. Electrolysis at the Potential of Peak B. The cell was loaded with dry THF (10 mL), Bu_4NPF_6 (0.8 g), $[Pd_3(dppm)_3(CO)](PF_6)_2$ (20 mg, 0.011 mmol), and Xyl−Br (200 mg, 0.563 mmol) under N_2. The potential was set to −1.25 V versus SCE, and the electrolysis stopped after the current dropped to zero (for a charge of 65 F/mol of cluster). The electrolysis product was purified as described. Isolated yield: 37%. The identity of the product was confirmed by the comparison of the spectroscopic data with an authentic sample.[12] ^{1}H NMR ($CDCl_3$): δ 6.36 (d, 1 H, H-1, ^3J(H-1, H-2) = 10.0 Hz), 5.75 (dd, 1 H, H-2, ^3J(H-2, H-3) = 4.4 Hz, ^3J(H-3, H-4) = 4.6 Hz), 5.28 (dd, 1 H, H-3, ^3J(H-3, H-4) = 4.6 Hz, ^3J(H-2, H-3) = 4.4 Hz), 5.16 (m, 1 H, H-4), 3.00−3.10 (m, 2 H, H-5a, H-5b), 2.08 (s, 3H, CH_3), 2.04 (s, 3H, CH_3). ^{13}C NMR ($CDCl_3$): δ 169.9, 169.8 (C=O), 125.8 (C-1), 117.2 (C-2), 66.7, 66.4 (C-3, C-4), 26.3 (C-5), 21.0, 20.9 (CH_3). Anal. Calcd for $C_9H_{12}O_4S$: C, 50; H, 5.66%. Found: C, 50.44; H, 5.70%.

(12) Bozo, E.; Boros, S.; Kunszmann, J. *Carbohydr. Res.* **1997**, *299*, 59.

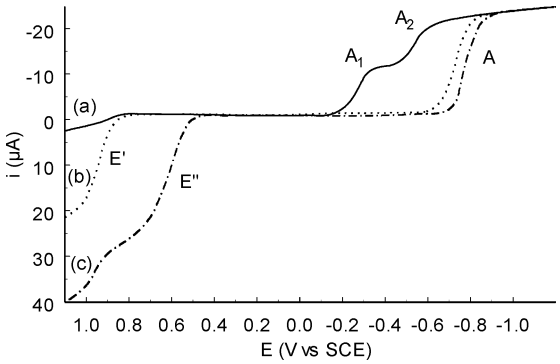

Figure 3. RDE voltammogram of 7.3 mM of Pd_3^{2+} (scan rate = 0.02 V/s) in 0.2 M THF−Bu_4NPF_6 solution at room temperature: (a) Pd_3^{2+} alone; (b) after addition of 1 equiv of Bu_4NBr; (c) after addition of 5 equiv of Bu_4NBr. Starting potential: +1.1 V.

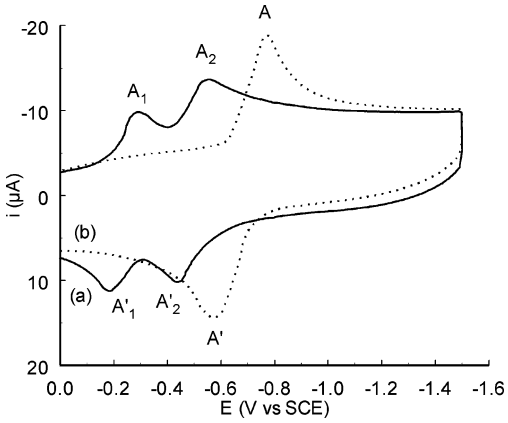

Figure 4. Cyclic voltammogram of 7.3 mM of Pd_3^{2+} (scan rate = 0.1 V/s) in 0.2 M THF−Bu_4NPF_6 solution at room temperature: (a) Pd_3^{2+} alone; (b) after addition of 1 equiv of Bu_4NBr. Starting potential: 0 V.

Results and Discussion

Reduction of Pd_3^{2+} and $Pd_3(Br)^+$. The voltammetric measurements using a rotating disk electrode (RDE) for the Pd_3^{2+} cluster, as a PF_6^- salt, in THF and in the presence of 0.2 M Bu_4NPF_6 as supporting electrolyte exhibit two reduction waves A_1 and A_2 at −0.29 and −0.51 V versus SCE (Figure 3, trace a). The cyclic voltammogram (CV) shows the same electrochemical processes as reversible systems (A_1/A'_1 and A_2/A'_2), which allows for the description of the following redox reactions (Figure 4, trace a).[13]

$$Pd_3^{2+} + e^- \rightleftharpoons Pd_3^{+} \ (A_1/A_1') \qquad (1)$$

$$Pd_3^{+} + e^- \rightleftharpoons Pd_3^{0} \ (A_2/A_2') \qquad (2)$$

The addition of 1 equiv of Bu_4NBr induces important modifications of the CV. The two reversible A_1/A'_1 and A_2/A'_2 systems become a single 2-electron peak A/A′ (Figure 4, trace b). Coulometric measurements indicate that 2 F/mol (n_{exp} = 2.06 F/mol) are consumed during the bulk electrolysis of $Pd_3(Br)^+$. The RDE voltammogram also shows the disappearance of the A_1 and A_2 reduction signals, and the appearance of A wave (Figure 3, trace b).[14] On the basis of ^{31}P NMR and these experiments, the reaction is quantitative

(13) Gautheron, I.; Mugnier, Y.; Hierso, K.; Harvey, P. D. *Can. J. Chem.* **1997**, *75*, 1182.

Scheme 1

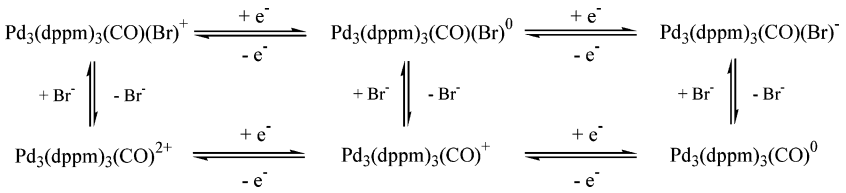

for the formation of the $Pd_3(Br)^+$ adduct as compared with an authentic sample.[15] The fast thermal reaction and electrochemical process are described as

$$Pd_3^{2+} + Br^- \rightarrow Pd_3(Br)^+ \quad (3)$$

$$Pd_3(Br)^+ + 2e^- \rightleftharpoons Pd_3^0 + Br^- \ (A/A') \quad (4)$$

Recently, our groups reported a detailed interpretation of the electrochemical behavior of the title cluster with I^- upon reduction as already stated.[5] In this case, a square scheme was used to describe the various mechanisms by which the Pd_3^{2+} cluster can be electrochemically reduced and reoxidized in the presence of I^- ions. The 2-electron reduction proceeds via two routes simultaneously. The first one involves two 1-electron reduction steps, followed by an iodide elimination to form the neutral Pd_3^0 cluster (EEC mechanism). In this work, the electrochemical behavior of the Pd_3^{2+}/Br^- system differs from that of Pd_3^{2+}/I^-, as shown later. The square scheme adapted for Br^- ions is presented in Scheme 1 in which the all ECE and EEC mechanisms can be depicted.

The reduction and reoxidation of Pd_3^{2+} in the presence of 5 equiv of Br^- ions induce a change in RDE voltammograms (Figure 3, trace c), where a 100 mV shift of wave A toward more cathodic potentials and the appearance of a new oxidation wave E″ at +0.65 V vs SCE are noted. The latter wave corresponds to the Br^- oxidation, as verified using Bu_4NBr alone. In the CV, the A/A′ wave is still present as previously found. With greater excess of Br^- (up to 20 equiv), no further modification in the intensity/potential curves of the cluster voltammograms is observed at room temperature. Upon cooling to −25 °C with 20 equiv of Br^- ions, a second electroreduction signal, A*, appears at −1.15 V versus SCE. When the sweep scan is increased, the intensity of wave A* increases with respect to wave A (Figure 5). These simple experiments give important insights regarding the interactions between the Br^- ions and the various Pd_3^{n+} species ($n = 0, 1, 2$) involved. Referring again to the square scheme, the dominant and unique species prior to reduction is $Pd_3(Br)^+$ on the basis of ^{31}P NMR data and literature binding constants.[11,16] The fact that only a single 2-electron wave is observed for the reduction of the $Pd_3(Br)^+$ starting material at room temperature indicates that

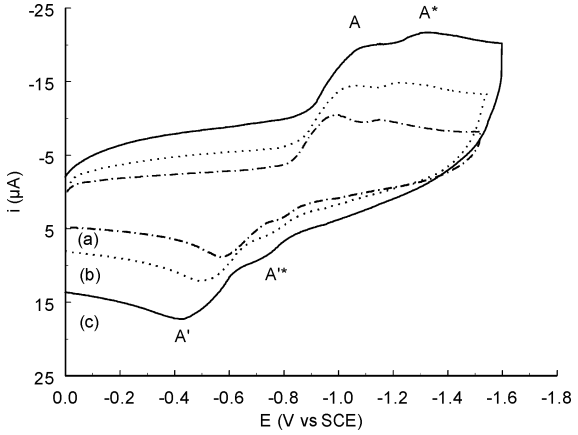

Figure 5. Cyclic voltammogram of 7.3 mM of Pd_3^{2+} in 0.2 M THF−Bu_4NPF_6 solution at −25 °C in the presence of 20 equiv of Bu_4NBr. Starting potential: 0 V. Scan rate: (a) 0.1 V/s, (b) 0.2 V/s, (c) 0.4 V/s.

an ECE mechanism exists, where the reduction potential of the Pd_3^+ species is less negative than that of $Pd_3(Br)^+$. The first reduction is followed by a rapid dissociation, and a rapid second 1-electron reduction occurs (ECE pathway in Scheme 1). However in the low temperature experiment, the presence of a large excess of Br^- ions provides evidence for a new process. Indeed, the lower temperature renders the dissociation less rapid, so that a second wave (A*) appears, which is associated with a second reduction of the $Pd_3(Br)^0$ unstable intermediate (EEC pathway in Scheme 1). At a faster scan rate, the $Pd_3(Br)^0$ species has less time to dissociate, hence promoting the reduction process. The latter species, $Pd_3(Br)^-$, is assumed to rapidly evolve to Pd_3^0.

All in all at room temperature, the electrochemical reduction of the $Pd_3(Br)^+$ species is dominated by an ECE mechanism while at lower temperature and in the presence of excess Br^- ions, an EEC mechanism now competes with the former. This behavior is similar to that of Pd_3^{2+} with I^- except that the EEC process is well observed at room temperature and without the use of an excess of I^-. This difference indicates that in fact the $Pd_3(Br)^0$ cluster dissociates more rapidly than the corresponding $Pd_3(I)^0$ species. This observation is consistent with the spectroscopically measured binding constants which indicate $K(I^-) > K(Br^-) > K(Cl^-)$ for the binding with Pd_3^{2+}.[16] Hence, the rapid dissociation of the $Pd_3(Br)^0$ adduct leads to a more efficient production of the radical species Pd_3^+. This preliminary study is important for the better understanding of the following reactivity between Pd_3^{n+} and the α- and β-Xyl−Br.

Stoichiometric Activation of Xyl−Br. The direct reaction of Pd_3^{2+} with α-Xyl−Br in a 1:1 ratio is easily monitored by CV, UV−vis, and ^{31}P NMR. The CVs exhibit a progressive evolution of the A_1/A'_1 and A_2/A'_2 waves in favor

(14) Wave E′ exhibits a similar intensity as A, suggesting a single 2-electron process as well.

(15) (a) Manojlovic-Muir, L. J.; Muir, K. W.; Lloyd, B. R.; Puddephatt, R. J. *J. Chem. Soc., Chem. Commun.* **1985**, 536. (b) Lloyd, B. R.; Manojlovic-Muir, L. J.; Muir, K. W.; Puddephatt, R. J. *Organometallics* **1993**, *12*, 1231.

(16) Harvey, P. D.; Hierso, K.; Braunstein, P.; Morise, X. *Inorg. Chem. Acta* **1996**, *250*, 337.

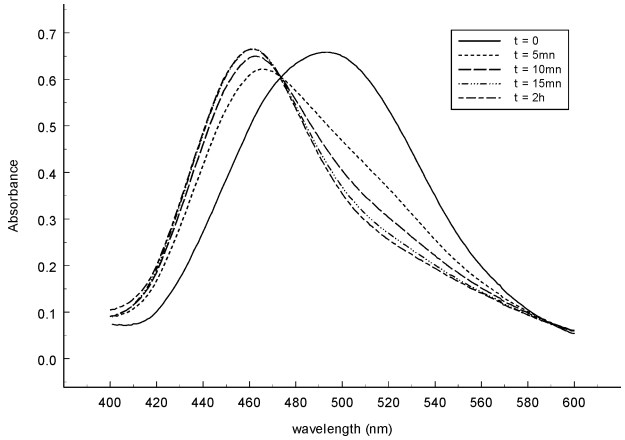

Figure 6. UV−vis spectral changes during the reaction of Pd_3^{2+} (2.88×10^{-5} M) with 45 equiv of α-Xyl−Br in THF.

of the A/A′ system known for the $Pd_3(Br)^+$ adduct, as confirmed by ^{31}P NMR and UV−vis spectroscopy (Figure 6), according to the following process:[17]

$$Pd_3^{2+} + Xyl{-}Br \rightarrow Pd_3(Br)^+ + \text{“}Xyl^+\text{”} \quad (5)$$

The C−Br activation can proceed via a dissociative or associative mechanism. The dissociative mechanism is described by eqs 6 and 7, while the associative one is described by eqs 8 and 9:[18]

$$Xyl{-}Br \underset{k_{-1}}{\overset{k_1}{\rightleftharpoons}} \text{“}Xyl^+\text{”} + Br^- \quad (6)$$

$$Pd_3^{2+} + Br^- \xrightarrow{k_3} Pd_3(Br)^+ \quad (7)$$

$$Xyl{-}Br + Pd_3^{2+} \underset{k_{-2}}{\overset{k_2}{\rightleftharpoons}} Pd_3(Xyl{-}Br)^{2+} \quad (8)$$

$$Pd_3(Xyl{-}Br)^{2+} \xrightarrow{k_4} Pd_3(Br)^+ + \text{“}Xyl\text{”} \quad (9)$$

The rates of reaction, for the dissociative (v_{diss}) and associative (v_{ass}) pathways, are given by eqs 10 and 11, respectively:[19]

$$v_{diss} = k_1[Xyl{-}Br] \quad (10)$$

$$v_{ass} = \frac{k_2 k_4 [Pd_3^{2+}][Xyl{-}Br]}{k_{-2} + k_4} = k[Pd_3^{2+}][Xyl{-}Br] \quad (11)$$

In the dissociative case, k_1 can be extracted from

$$\ln([Xyl{-}Br]/[Xyl{-}Br]_0) = -k_1 t \quad (12)$$

where $[Xyl{-}Br]_0$ and $[Xyl{-}Br]$ are the concentrations of Xyl−Br at $t = 0$, and at a given time.[19]

(17) “Xyl^+” is assumed to evolve, but no attempt was made to identify the organic products due to the small amount used in stoichiometric conditions, and in the presence of a large excess of supporting electrolyte.

(18) A dissociative mechanism is plausible in this case since “Xyl^+” is stabilized by resonance involving delocalization of the S atom lone pair.

(19) The demonstration for eqs 10−14 is provided in the Supporting Information.

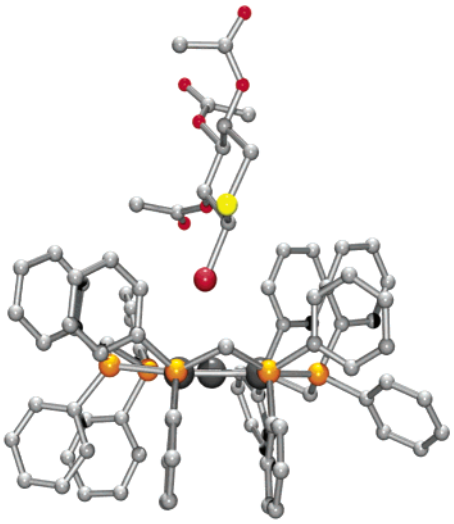

Figure 7. Example of a computed ball-and-stick model of the $Pd_3^{2+}\cdots$ β-Xyl−Br host−guest system. The H-atoms and CO group are not shown.

In the associative case, a linear relationship is predicted if $[Xyl{-}Br]_0 > [Pd_3^{2+}]_0$, according to

$$\frac{1}{[Pd_3^{2+}]_0 - [Xyl{-}Br]_0} \ln \frac{[Pd_3^{2+}]_0[Xyl{-}Br]}{[Xyl{-}Br]_0[Pd_3^{2+}]} = -kt \quad (13)$$

where $[Pd_3^{2+}]_0$ and $[Pd_3^{2+}]$ are the concentrations of Pd_3^{2+} at $t = 0$ and at a given time, as well.[19]

If $[Xyl{-}Br]_0 = [Pd_3^{2+}]_0$, then

$$\frac{1}{[Pd_3^{2+}]} - \frac{1}{[Pd_3^{2+}]_0} = kt \quad (14)$$

The $[Xyl{-}Br]$ and $[Pd_3^{2+}]$ quantities can be evaluated from the intensities of the A_1 peak in the CV of the reacting mixture. The application of eq 14 leads to a straight line with $k = 76.4$ L·mol^{-1}·min^{-1}, where $R^2 = 0.9984$ (Supporting Information). The data do not lead to a linear relation using eq 12 (Supporting Information), so these results indicate an associative mechanism.

The β-Xyl−Br also reacts with Pd_3^{2+} in a 1:1 ratio to form $Pd_3(Br)^+$. However, this reaction is immediate, so no kinetic data could be extracted. Intuitively, the Br^- ion is a better leaving group in the α-isomer because of the periplanar geometry of the S lone pair and the C−Br bond. This difference of rate of C−Br bond activation ($\beta > \alpha$) can be explained by steric hindrance. Computer modeling indicates that the approach of the Br atom inside the cavity for β-Xyl−Br is easier (Figure 7), while the $Pd_3^{2+}\cdots$α-Xyl−Br interactions are more hindered (Figure 8). The qualitative results for these computations are that the β-isomer always exhibits closer Br···Pd distances for the various orientations of the substrate in the cavity. The closest computed contact is 3.04 Å, which differs significantly from the closest one found for the α-isomer (d(Br···Pd) = 3.18 Å). These distances are well located within the sum of the van der Waals radii (r_{vdw} = 1.60 Å (Pd), 1.90 Å (Br)),[20] and therefore, the presence of reactivity is not surprising. These findings corroborate recent studies on the photochemical oxidation of Pd_3^{2+} in

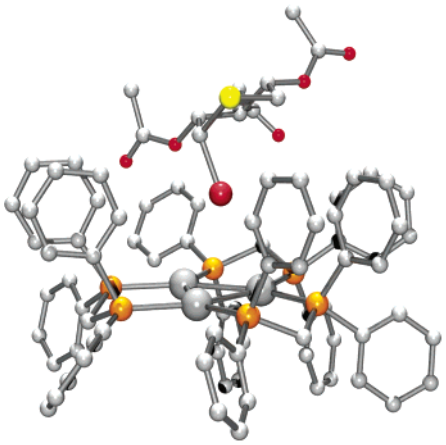

Figure 8. Example of a computed ball-and-stick model of the $Pd_3^{2+}\cdots$ α-Xyl−Br host−guest system. The H-atoms and CO group are not shown.

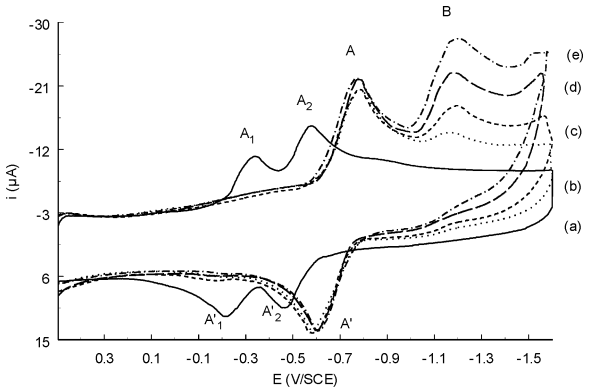

Figure 9. Cyclic voltammogram of 7.3 mM of Pd_3^{2+} (scan rate = 0.1 V/s) in 0.2 M THF−Bu_4NPF_6 solution at room temperature: (a) Pd_3^{2+} alone. Parts b−e show the effect of addition of β-Xyl−Br: (b) 1 equiv, (c) 5 equiv, (d) 20 equiv, (e) 50 equiv. Starting potential: +0.5 V.

the presence of chlorocarbons, where rates of reactivity (i.e., quantum yields) were functions of the substrate dimension.[21]

In order to stress the importance of the host−guest interactions, this C−Br bond activation reactivity is also investigated with the $Pd_3(CF_3CO_2)^+$ species. Previous X-ray studies show that the $CF_3CO_2^-$ anion is located inside the cavity in the cluster $[Pd_3(dppm)_3(CO)(CF_3CO_2)](PF_6)$ while the cavity is empty in $[Pd_3(dppm)_3(CO)](PF_6)_2$.[11] The Pd••O distances witness the presence of strong ionic interactions. Binding constant measurements from UV−vis data show that RCO_2^- species bind weakly and reversibly to the Pd_3^{2+} species, while PF_6^- does so to a lesser degree or not at all.[11,22] Despite these small constants for the RCO_2^- species, neutral molecules exhibit even weaker constants, which suggests that, in stoichiometric amounts, neutral substrates have little chance to penetrate the cavity when the "blocking" $CF_3CO_2^-$ counterion is used. In a 1:1 ratio, both α- and β-Xyl−Br are found to be unreactive toward $Pd_3(CF_3CO_2)^+$, even after several hours. When this ratio is changed to 1:5 ($Pd_3(CF_3CO_2)^+$/Xyl−Br), a partial and slow conversion of $Pd_3(CF_3CO_2)^+$ into $Pd_3(Br)^+$ is observed after a few hours. This result illustrates the effect of host−guest interactions between the Pd_3^{2+} and $CF_3CO_2^-$ on the heterolytic cleavage reactivity.

However, in a stoichiometric mixture, the concentration of the neutral substrate Xyl−Br is not great enough to compete with the counterion to occupy the cavity. Therefore, a greater concentration is required, and this conclusion further demonstrates the associative mechanism for the C−Br activation by the cluster species Pd_3^{2+} as either a PF_6^- or $CF_3CO_2^-$ salt (with the PF_6^- system being more efficient). The use of Pd_3^{2+} to promote (host−guest) reactivity with a glycoside is, to our knowledge, unprecedented.[23]

Electrocatalysis. The electrochemical investigations under stoichiometric conditions lead to the obvious difficulty of identification and separation of the organic products, due to the low amount of materials relative to the supporting electrolyte. In addition, the 2-electron reduction of Pd_3^{2+} provides the highly reactive species Pd_3^0, which can activate R−Br species but also does not show affinity for Br^- ions as shown, hence providing a way to regenerate the catalyst. The Pd_3^0 catalytic activity toward α-Xyl−Br activation is now presented and will be denoted as Xyl−Br.[24]

Because Pd_3^{2+} reacts with Xyl−Br to form $Pd_3(Br)^+$ (eq 5), the electrolyses are performed at potentials corresponding to wave A. In this manner, the Pd_3^0 is generated efficiently, releasing Br^- (eq 4). Figure 9 shows the CV of Pd_3^{2+} alone and with 1 equiv of Xyl−Br (curves a and b). As anticipated under these stoichiometric conditions, the conversion is complete. When more equivalents of Xyl−Br are added to the solution, the A/A′ system is not perturbed but a new peak (B) increases ($E_p = -1.17$ V vs SCE) proportionally to the added amount of substrates (curves c−e). The generated Pd_3^0 species reacts slowly with Xyl−Br to form a new species, which is reduced at peak B. Because this second reduction leads to Pd_3^0 again, the reoxidation wave A′ is not altered. The thin layer CV measurements exhibit the same behavior, excluding the possibility that a reaction between the species electrogenerated at peak B and starting material $Pd_3(Br)^+$ occurs.

Electrocatalysis at Wave A. The electrolysis of $Pd_3(Br)^+$ in the presence of 18 equiv of Xyl−Br at wave A ($E_p = -0.9$ V vs SCE) consumes 20 F/mol of cluster. The electrolysis is accompanied by a decrease and increase of waves A and B, respectively (Figure 10). After total electrolysis, wave A has disappeared, and wave B exhibits a peak-current quasi-identical to that of wave A initially, suggesting that the resulting product also exhibits a 2-electron reduction process at wave B.[25] The ^{31}P NMR of the resulting

(20) *Basic Inorganic Chemistry*; Cotton, F. A., Wilkinson, G., Eds.; John Wiley & Sons: New York, 1980; p 61.
(21) Harvey, P. D.; Provencher, R.; Gagnon, J.; Zhang, T.; Fortin, D.; Hierso, K.; Drouin, M.; Socol, S. M. *Can. J. Chem.* **1996**, *74*, 2268.
(22) (a) The PF_6^- anion has been found inside the larger cavity of $Pd_3(dpam)_3(CO)^{2+}$ (dpam = $(Ph_2As)_2CH_2$).[22b] (b) Zhang, T.; Drouin, M.; Harvey, P. D. *J. Chem. Soc., Chem. Commun.* **1996**, 877.
(23) (a) Unpublished results show that Pd_3^{2+} participates in the Br^- substitution of α-Xyl−Br by thiolate anions (RS^-; R = Ar), where the major product (Xyl−SR) exhibits an inversion of configuration (α/β ratio = 20/80). In the absence of Pd_3^{2+}, a slow reactivity is noted with a racemic product distribution (α/β ratio = 50/50). Such a result can only be explained by an associative mechanism where a great amount of $Pd_3^{2+}\cdots$Br−Xyl exists.[23b] (b) Brevet, D. Ph.D. Thesis, Université de Bourgogne, Dijon, France, 2002.
(24) β-Xyl−Br is slightly unstable in solution, so long term electrochemical experiments are altered by this instability.
(25) The product is EPR silent.

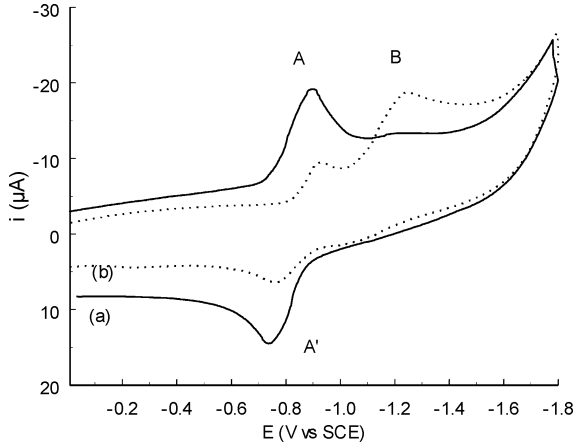

Figure 10. Cyclic voltammogram of 7.3 mM of $Pd_3(Br)^+$ at $\upsilon = 0.1$ V/s in 0.2 M THF−Bu_4NPF_6 solution at room temperature: (a) $Pd_3(Br)^+$ in the presence of 18 equiv of Xyl−Br; (b) after reduction at −0.95 V and consumption of 20 F.

Scheme 2

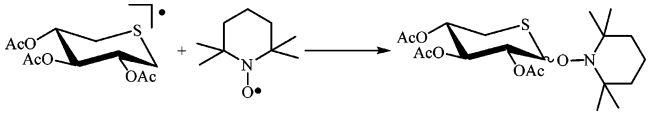

solution shows a single signal at −2.57 ppm, which disappears with time, illustrating the limited stability of the electrochemical inorganic product (or intermediate). The isolated yields for the organics are 79% for Xyl−H and 12% for the 3,4-di-*O*-acetyl-5-thioxylal.[26] The former can only be explained by the formation of the free radical "Xyl•" which abstracts H• from the solvent. THF is known to be a source of H•.[27,28] The generation of a radical species from $Pd_3(Br)^+$ must proceed according to

$$\text{Xyl}-\text{Br} + 1e^- \xrightarrow{Pd_3(Br)^+(\text{cat.})} \text{“Xyl}^\bullet\text{”} + Br^- \qquad (15)$$

The existence of "Xyl•" is proven using the well-known spin trap reagent agent TEMPO (2,2,6,6-tetramethylpiperiin-1-oxyl).[29] In the presence of TEMPO, this same electrolysis leads to the *O*-glycosylation Xyl−TEMPO product with an isolated yield of 70% according to the reaction described in Scheme 2.

Similarly, monitoring the coupling reaction between Xyl• and DMPO (5,5′-dimethyl-1-pyrroline *N*-oxide)[30] by EPR allows one to detect the coupling product Xyl−DMPO (Figure 11, Scheme 3).

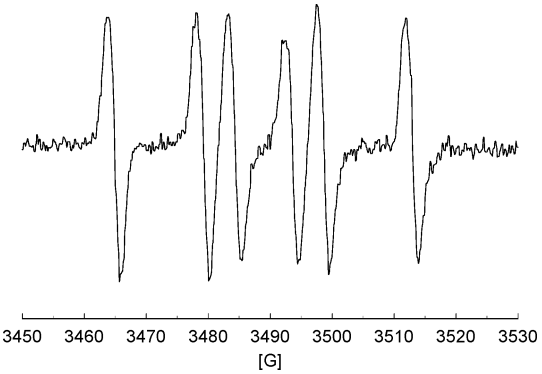

Figure 11. EPR spectrum resulting from the coupling reaction between Xyl• and DMPO ($a_N = 14.25$ G; $a_H = 19.34$ G; $g = 2.008$).

Scheme 3

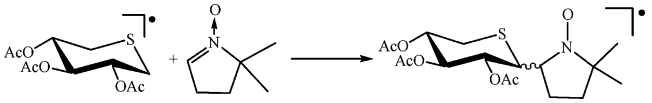

Scheme 4

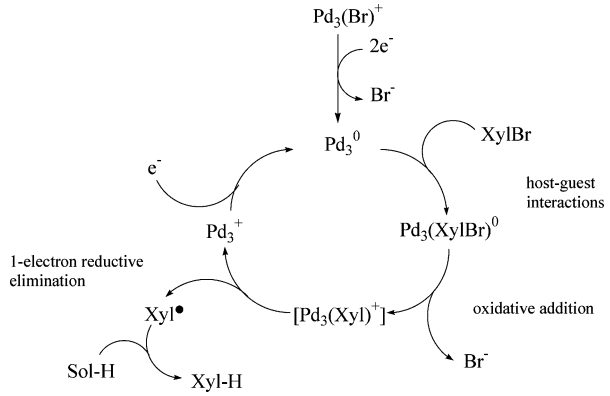

The EPR spectrum shows the anticipated doublet of triplet characteristic of hyperfine coupling with the N and H atoms (Figure 11).[31] The proposed catalytic cycle is shown in Scheme 4.

The 2-electron reduction of $Pd_3(Br)^+$ precatalyst leads to the highly reactive zerovalent Pd_3^0. Interactions with Xyl−Br generate a host−guest complex $Pd_3(Xyl-Br)^0$. The oxidative addition of this substrate onto the Pd_3^0 center forms an intermediate that is speculatively formulated as $Pd_3(Xyl)^+$ (reducible at wave B). The proposal is based on the information collected and already described here. The ^{31}P NMR datum (−2.57 ppm) is in the same range as those found for Pd_3^{2+} (−1.25 ppm) and $Pd_3(Br)^+$ (−6.14 ppm). The compound is also EPR inactive, and electrochemical observations suggest that wave B is a 2-electron process (i.e., similar to $Pd_3(Br)^+$). The more negative potential of wave B is consistent with the better σ-donor property of the carbonium ion. Then, a 1-electron reductive elimination occurs to generate the observed Xyl• intermediate and Pd_3^+, which is rapidly reduced to Pd_3^0 at this more negative potential (than that of Pd_3^+/Pd_3^0; wave A_2). This irreversible reaction drives the catalysis. The free radical species is well-

(26) At the end of the electrolysis, the solvent was removed, and the residue was extracted with Et_2O. The products were separated and isolated by column chromatography on silica gel. The overall isolated yield is 91%.

(27) Peters, D. G. In *Organic Electrochemistry*, 3rd ed., revised and expanded; Lund, H., Baiser, M. M., Dekker, M., Eds.; INC: New York, 1992; p 361.

(28) Nishino, T.; Watanabe T.; Okada, M.; Nishiyama, Y.; Sonoda, N. *J. Org. Chem.* **2002**, *67*, 966.

(29) (a) *Organic Chemistry of Stable Free Radicals*; Forrester, A. R., Hay, J. M., Thomson, R. H., Eds.; Academic Press: London, 1968. (b) Rozantsev, E. G. In *Free Nitroxyl Radicals*; Ulrich, H., Ed.; Plenum Press: New York, 1970. (c) *Spin Labeling. Theory and Application*; Berliner, L. J., Ed.; Academic Press: New York, 1976. (d) Yamago, S.; Miyazoe, H.; Yoshida, J. *Tetrahedron Lett.* **1999**, *40*, 2339.

(30) Rota, C.; Barr, D. P.; Martin, M. V.; Guengerich, F. P.; Tomasi, A.; Mason, R. P. *Biochem. J.* **1997**, *328*, 565.

(31) Witting, P. K.; Travascio, P.; Sen, D.; Mauk, A. G. *Inorg. Chem.* **2001**, *40*, 5017.

Scheme 5

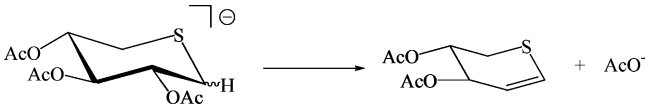

Scheme 6

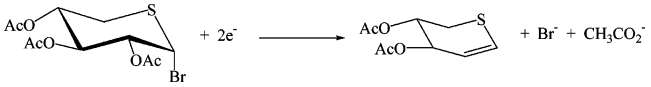

known to abstract H• from THF[27,28] and explains the presence of the major product.[32]

The presence of 3,4-di-*O*-acetyl-5-thioxylal (12%) results from the generation of Xyl^-, which is unstable (Scheme 5). Indeed, this anion species readily eliminates acetate ions.[33,34] At higher negative potentials, this amount of 12% increases (see later).

This second reaction requires 2 F/mol, and the experimental result of 20 F is consistent with the mechanism for the 1-electron process (Scheme 4), and the 2-electron reduction (presented in a following paragraph). This 20 F accounts for 2 electrons for the generation of the Pd_3^0 catalyst, 14 electrons to produce the major Xyl−H product, and 4 electrons to produce the minor Xyl^- intermediate responsible for the 3,4-di-*O*-acetyl-5-thioxylal.

Electocatalysis at Wave B. The bulk electrolysis of $Pd_3(Br)^+$ in the presence of 50 equiv of Xyl−Br at peak B (−1.25 V vs SCE) leads to completion after consumption of 65 F. The isolated yield for thioxylal is 37%, which is identified by mass spectrometry and NMR (^1H, ^{13}C). There is no evidence for Xyl−H, excluding the radical-type mechanism in this case. The overall reaction is described in Scheme 6.

The important difference is that, at a higher negative potential, the $Pd_3(Xyl)^+$ intermediate is readily reduced with 2 electrons to generate Xyl^- and Pd_3^0. The catalytic cycle is shown in Scheme 7. The overvoltage for the reduction of Xyl−Br is decreased by 0.55 V when the Pd_3^{2+} catalyst is used. This mechanism is similar to that shown in Scheme 4 where a 2-electron reduction of $Pd_3(Br)^+$ leads to Pd_3^0. Host−guest interactions generate the same supramolecular assembly

Figure 12. Drawing of β-Xyl−OAc.

Scheme 7

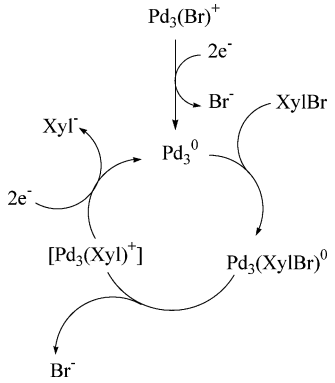

$Pd_3(Xyl-Br)^0$. Subsequently, the oxidative addition generates the anticipated $Pd_3(Xyl)^+$ intermediate. Because the electrolysis is performed at a more negative potential, $Pd_3(Xyl)^+$ is further reduced to form the carbanion and regenerate Pd_3^0. Finally, as already stated, Xyl^- evolves to the thioxylal, excluding the formation of the radical Xyl•. The low 37% yield is due, in part, to a secondary reaction involving a nucleophilic attack from the produced AcO^- anion onto the starting material α-Xyl−Br to produce β-Xyl−OAc (Figure 12) and Br^-.[33] Such a process is not uncommon for such substrates[33b] and may account for the coulometric consumption of 65 F, while the bielectronic reduction of the introduced quantity of Xyl−Br would theoretically require 100 F.

Exhaustive investigations are clearly needed in order to improve yields (effect of the reduction potential, temperature, and solvent).

Concluding Remarks

The Pd_3^{2+} abstracts the Br atom in Xyl−Br via an associative process in the cavity of the Pd_3^{2+} cluster, to generate $Pd_3(Br)^+$ and "Xyl^+". This work also shows that the Br^- ion can be labilized from a 2-electron reduction of $Pd_3(Br)^+$ via an ECE mechanism at room temperature, and that this electrogeneration forms the Pd_3^0 species which can activate the C−Br bond in Xyl−Br. This conversion of Xyl−Br into Xyl^- can be rendered catalytic which opens the door to useful applications in glycoside and organic chemistry. This work also shows that the potential control leads to the Xyl• and Xyl^- intermediates. The chemistry related to Xyl•, which can only be generated with the presence of Pd_3^{2+},[35] is fascinating and certainly deserves a closer look. In addition, yield improvements for the generation of Xyl^-, as well as eliminating undesired side reactions, will be the subject of further research. The presence of the supramolecular assembly $Pd_3(XylBr)$ provides an opportunity to attain selectivity in the catalytic Br-substitution reactions (SN_1 vs SN_2

(32) (a) The importance of radical reactions in organic synthesis has recently increased, since functional group conversion of organic compounds under mild conditions is critical for the preparation of natural products and fine chemicals.[32b−d] In particular, the coupling reaction of a sugar anomeric radical with electron poor heteroaromatic bases is effective for the synthesis of C-nucleosides.[32e−h] The addition of glycoside radicals to α,β-unsaturated carbonyl compounds has been developed by Giese et al. as a practical method for the synthesis of C-glycosides.[32i] (b) *Free Radicals in Organic Chemistry*; Fossey, J., Lefort, D., Sorba, J., Eds.; John Wiley & Sons: Paris, 1995. (c) *Radicals in Organic Synthesis: Formation of Carbon−Carbon Bonds*; Giese, B., Ed.; Pergamon Press: Oxford, 1986. (d) *Free Radical Chain Reactions in Organic Synthesis*; Motherwell, W. B., Crich, D., Ed.; Academic Press: New York, 1992. (e) Togo, H.; Fujii, M.; Ikuma, T.; Yokoyama, M. *Tetrahedron Lett.* **1991**, *32*, 3377. (f) Togo, H.; Ishigami, S., Yokoyama, M. *Chem. Lett.* **1992**, 1673. (g) Togo, H.; Ishigami, S.; Yokoyama, M. *J. Chem. Soc., Perkin Trans. 1* **1994**, 2407. (h) Togo, H.; Ishigami, S.; Fujii, M.; Ikuma, T. Yokoyama, M. *J. Chem. Soc., Perkin Trans. 1* **1994**, 2931. (i) For a review see: Giese, B. *Angew. Chem., Int. Ed. Engl.* **1989**, *28*, 969.

(33) (a) The side products were observed. (b) Maran, F.; Vianello, E.; Catelani, G.; D'Angeli, F. *Electrochim. Acta* **1989**, *34*, 587.

(34) Brevet, D.; Mugnier, Y.; Samreth, S. Submitted for publication.

(35) The direct electrolysis of Xyl−Br ($E_p = -1.8$ V) leads only to the formation of Xyl^-.[23b,34]

mechanism). Indeed, preliminary results show that Pd_3^{2+} acts as a strong Lewis acid promoting inversion of configuration in both α- and β-Xyl−Br.[23]

Acknowledgment. P.D.H. thanks NSERC (Natural Sciences and Engineering Research Council) for funding. Y.M. is grateful to the "Conseil Regional de Bourgogne" and "Laboratoire Fournier SA" for funding (Bourse D. B. et contrats d′études n*o*. 00/5112/A1/00023 et 01/5162/S4/00023), and to M. T. Compain for her important technical assistance.

Supporting Information Available: Graph showing $(1/[Pd_3^{2+}]) - (1/[Pd_3^{2+}]_0)$ versus time, graph showing $\ln([Xyl-Br]/[Xyl-Br]_0)$ versus time, UV−vis spectra of Pd_3^{2+} in the presence of Xyl−OAc versus time, demonstrations of eqs 10−14. This material is available free of charge via the Internet at http://pubs.acs.org.

IC026279X